ISSN 0031-918X, Physics of Metals and Metallography, 2017, Vol. 118, No. 6, pp. 579–590. © Pleiades Publishing, Ltd., 2017.
Original Russian Text © D.G. Shaysultanov, N.D. Stepanov, G.A. Salishchev, M.A. Tikhonovsky, 2017, published in Fizika Metallov i Metallovedenie, 2017, Vol. 118, No. 6, pp. 610–621.

STRUCTURE, PHASE TRANSFORMATIONS, AND DIFFUSION

Effect of Heat Treatment on the Structure and Hardness of High-Entropy Alloys $CoCrFeNiMnV_x$ ($x = 0.25, 0.5, 0.75, 1$)

D. G. Shaysultanov[a], *, N. D. Stepanov[a], G. A. Salishchev[a], and M. A. Tikhonovsky[b]

[a] *Belgorod National Research University, ul. Pobedy 85, Belgorod, 308015 Russia*

[b] *Kharkov Institute of Physics and Technology, ul. Akademicheskaya 1, Kharkov, 61108 Ukraine*

* *e-mail: shaysultanov@bsu.edu.ru*

Received October 3, 2016; in final form, December 13, 2016

Abstract—High-entropy alloys $CoCrFeNiMnV_x$ ($x = 0.25, 0.5, 0.75, 1$) were prepared by vacuum arc melting. The structure and microhardness of the alloys have been studied in the cast state and after annealing at temperatures of 700–1100°C. It has been found that the alloys consist of the fcc (γ) solid solution and intermetallic sigma (σ) phase. The volume fraction of the σ phase increases with increasing vanadium content. As a result of annealing, phase transformations occur, including the precipitation of σ particles from the γ phase and, vice versa, the precipitation of γ particles from the σ phase. It has been shown that the change in the volume fraction of the σ phase upon annealing occurs due to the changes in the total content of σ-forming elements, chromium and vanadium, in accordance with the lever rule. With increasing temperature, the volume fraction of the σ phase varies nonmonotonically; first, it increases, then it decreases. The microhardness of the alloys correlates well with the change in the volume fraction of the σ phase. The mechanisms of the phase transformations and quantitative relationships between chemical and phase compositions of the alloys and their hardness are discussed.

Keywords: high-entropy alloys, heat treatment, microstructure, σ phase

DOI: 10.1134/S0031918X17060084

INTRODUCTION

High-entropy alloys (HEAs) are usually defined as alloys that consist of five or more elements with approximately equiatomic concentrations [1]. A large number of elements taken in equal proportions should increase the entropy of mixing of the disordered substitutional solid solution, thereby presumably making their formation thermodynamically more preferred than the formation of intermetallic phases [1]. However, further studies have shown that the high entropy of mixing is not a determining factor in the phase formation of multicomponent alloys [2]. In many HEAs, complicated multiphase structures with a large volume fraction of ordered and/or intermetallic phases are formed [3–6]. From the viewpoint of possible practical applications, the presence of strengthening second phases is attractive in order to provide a desired level of mechanical properties. However, this requires controlling the volume fraction, morphology, and dispersion of second phases using alloying, heat, and thermomechanical treatments. In particular, the lack of data on the regularities of phase transformations in these multicomponent alloys makes it difficult to develop practically important compositions and regimes of their treatment.

One of the commonly occurring intermetallic phases detected in HEAs is the σ phase [7]. In particular, the σ phase is detected in some multicomponent alloys that contain chromium and vanadium, including $Al_xCrFe_{1.5}MnNi_{0.5}$ [8], CoCrFeNiV [9], $CoCrFeNiMnV_x$ [10], $Al_{0.5}CoCrCuFeNiV_x$ [11], and others [12]. The σ phase is a topologically close-packed phase with a tetragonal structure and is known for its high hardness [13]. Its precipitation can lead to the embrittlement of, e.g., stainless steels or nickel superalloys [14]. On the other hand, the observed strengthening of $CoCrFeNiMnV_x$ [10] or $Al_{0.3}CrFe_{1.5}MnNi_{0.5}$ [8] alloys due to the formation of the σ phase shows that the σ phase can be used to increase strength characteristics. In both cases, if the σ phase embrittles or strengthens the alloy, it is important to control its precipitation or dissolution upon heat treatment. Meanwhile, for HEAs prone to the formation of the σ phase, the effect of the heat-treatment conditions on the phase composition and microstructure have only been studied weakly. The authors of [15] studied the effect of the aging conditions on the structure and properties of the $Al_{0.3}CrFe_{1.5}MnNi_{0.5}$ alloy and detected the precipitation of the σ phase at temperatures of 650 and 750°C. The formation of the σ phase after annealing at 700°C was revealed also in

Chemical composition of ingots of $CoCrFeNiMnV_x$ alloys ($x = 0.25, 0.5, 0.75, 1$)

Alloy	Elemental composition, at %					
	Co	Cr	Fe	Ni	Mn	V
$CoCrFeNiMnV_{0.25}$	19.3	20.0	19.6	19.5	17.0	4.6
$CoCrFeNiMnV_{0.5}$	18.9	18.8	18.4	18.0	17.8	9.1
$CoCrFeNiMnV_{0.75}$	17.2	17.5	18.2	17.2	16.5	13.3
$CoCrFeNiMnV_1$	16.2	17.0	17.2	16.5	16.1	17.0

the $Al_xCrFe_{1.5}MnNi_{0.5}$ alloys [16]. However, the studies carried out do not give a complete picture of phase equilibria in these alloys.

In the present paper, $CoCrFeNiMnV_x$ alloys with $x = 0.25$, 0.5, 0.75, and 1 were chosen as the material for study. Earlier, the authors of [10] have studied the effect of the V concentration on the structure and mechanical properties of these alloys. The alloys consisted of mixtures of γ solid solution and tetragonal σ phase enriched in chromium and vanadium. In the homogenized state (after annealing at 1000°C for 24 h), the $CoCrFeNiMnV_{0.25}$ alloy contained 2% σ phase; in the CoCrFeNiMnV alloy, 72% σ phase was detected. Due to the pronounced effect of the vanadium content on the phase composition of the $CoCrFeNiMnV_x$ alloys, it can be supposed that the study of their phase stability can give new data on the conditions of the formation of the σ phase in multi-element alloys. In the present paper, we studied the structure and hardness of the $CoCrFeNiMnV_x$ alloys ($x = 0.25$, 0.5, 0.75, 1) after heat treatments in the temperature range of 700–1100°C.

EXPERIMENTAL

The $CoCrFeNiMnV_{0.25}$, $CoCrFeNiMnV_{0.5}$, $CoCrFeNiMnV_{0.75}$, and $CoCrFeNiMnV_1$ alloys were prepared by vacuum arc melting in high-pure argon with subsequent casting in a water-cooled copper mold. The purity of the alloying elements was above 99.9 at %. To ensure chemical homogeneity, the ingots were remelted at least five times. The cooling rate of the ingots to 800°C was equal to 50 K/s. The chemical composition of the alloys is presented in the table.

Ingots of the CoCrFeNiMn and $CoCrFeNiMnV_1$ alloys had dimensions of 6 × 15 × 60 mm, while ingots of the $CoCrFeNiMnV_{0.25}$, $CoCrFeNiMnV_{0.5}$, and $CoCrFeNiMnV_{0.75}$ alloys had dimensions of 6 × 8 × 45 mm. Samples with dimensions of 6 × 8 × 3 mm were cut from ingots to use for subsequent annealing at temperatures of 700, 800, 900, 1000, and 1100°C for 24 h. The upper temperature boundary of the heat treatment was chosen based on the data of a differential scanning calorimetry (DSC), which showed that the solidus temperature of the alloys is about 1200°C. The samples were sealed in an evacuated (10^{-2} Torr) quartz tube filled with titanium chips to prevent oxidation. The cooling of the samples from the annealing temperature was carried out in water. The DSC was performed using a NETZSCH device in a helium atmosphere; the rates of heating and cooling of the samples were 20 K/min.

The alloys were studied in the cast and heat-treated states. The microstructure and the phase composition of the alloys were studied using X-ray diffraction analysis, scanning electron microscopy (SEM), and transmission electron microscopy (TEM). The X-ray diffraction analysis was carried out using a RIGAKU diffractometer in Cu $K\alpha$ radiation in the range of angles of 25–125°. The SEM study of the microstructure was performed using a Quanta 200 3D microscope, which was equipped with a detector of backscattered electrons and with attachments for the energy-dispersive X-ray analysis (EDS) and for processing maps of electron backscatter diffraction (EBSD). Samples for TEM analysis, which were mechanically prethinned to 100 μm, were prepared by electropolishing using a TenuPol-5 device in a mixture of C_2H_5OH (95%) and $HClO_4$ (5%). The study of the fine structure of the alloys was carried out using a JEOL JEM-2100 electron microscope, which was equipped with an attachment for EDS analysis.

RESULTS

The microstructure of the $CoCrFeNiMnV_x$ alloys ($x = 0.25$, 0.5, 0.75, 1) in the cast state is presented in Fig. 1. It can be seen that the microstructure changes significantly depending on the vanadium content. In the $CoCrFeNiMnV_{0.25}$ alloy, a single-phase (γ) structure (Fig. 1a) is observed, which is confirmed by the TEM data [10]. The increase in the vanadium concentration to $x = 0.5$ leads to the appearance of particles of the σ phase that have a lighter contrast in the SEM images (Fig. 1b). A further increase in the vanadium content leads to an increase in the volume fraction of particles of the σ phase (Fig. 1c). At the maximum vanadium concentration, the σ phase becomes dominating. The γ phase is in the form of (i) precipitates at the grain boundaries of the σ phase, and (ii) fine platelike and/or equiaxed precipitates within the grains of the σ phase (see the inset in Fig. 1d corresponding to a higher magnification) [10]. The TEM method allowed us to

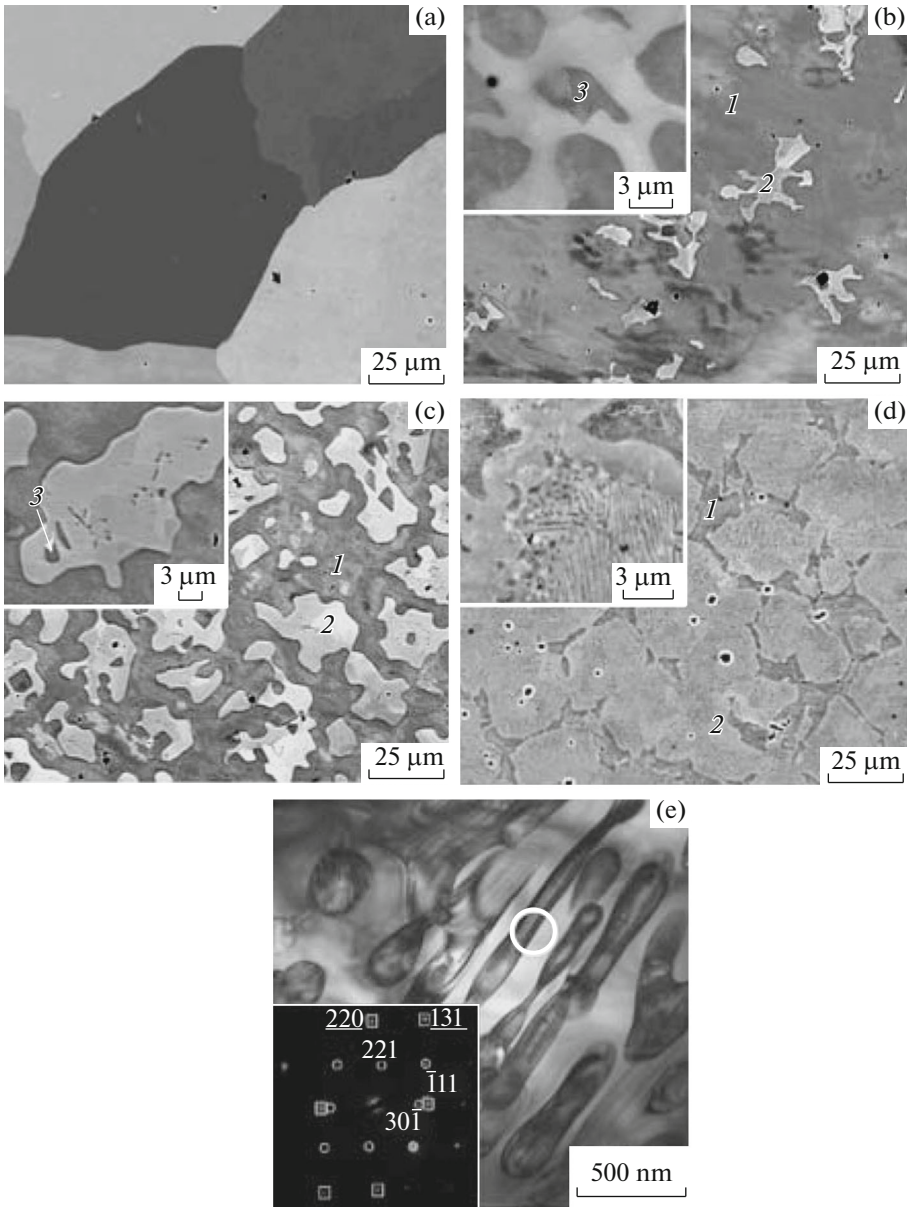

Fig. 1. Microstructure of the $CoCrFeNiMnV_x$ alloys in the cast state. SEM images: (a) $x = 0.25$; (b) $x = 0.5$; (c) $x = 0.75$; and (d) $x = 1$. TEM image: (e) $x = 1$. (*1*, *3*) γ phase; (*2*) σ phase.

found that for the platelike γ precipitates in coarse σ particles, the following orientation relationships are fulfilled: $(\bar{1}11)_\gamma \| (30\bar{1})_\sigma$ and $[\bar{2}2\bar{4}]_\gamma \| [2\bar{5}6]_\sigma$. Note that, as a rule, the particles of the σ phase in the $CoCrFeNiMnV_{0.5}$ and $CoCrFeNiMnV_{0.75}$ alloys have an irregular shape with wavy branched interfaces with the γ phase and contain particles of an equiaxed or platelike shape depending on the vanadium concentration in the other phase.

The microstructure of the $CoCrFeNiMnV_{0.25}$ alloy after heat treatment at different temperatures is presented in Fig. 2. Annealing at a temperature of 700°C leads to the formation of particles at the grain boundaries (denoted by *2* in Fig. 2a). The increase in the amount and size of particles with increasing temperature to 900°C is observed (Figs. 2b, 2c). However, after annealing at 1000 and 1100°C, no particles are detected. Because of the low volume fraction of these particles, they cannot be identified using the X-ray diffraction method, but the use of the local EDS and EBSD analysis [10] made it possible to reliably identify these particles as the tetragonal chromium- and vanadium-rich σ phase.

Figure 3 shows the changes in the microstructure of the $CoCrFeNiMnV_{0.5}$ alloy upon an increase in the annealing temperature. It should be noted that the study of the phase composition of the alloy using X-ray

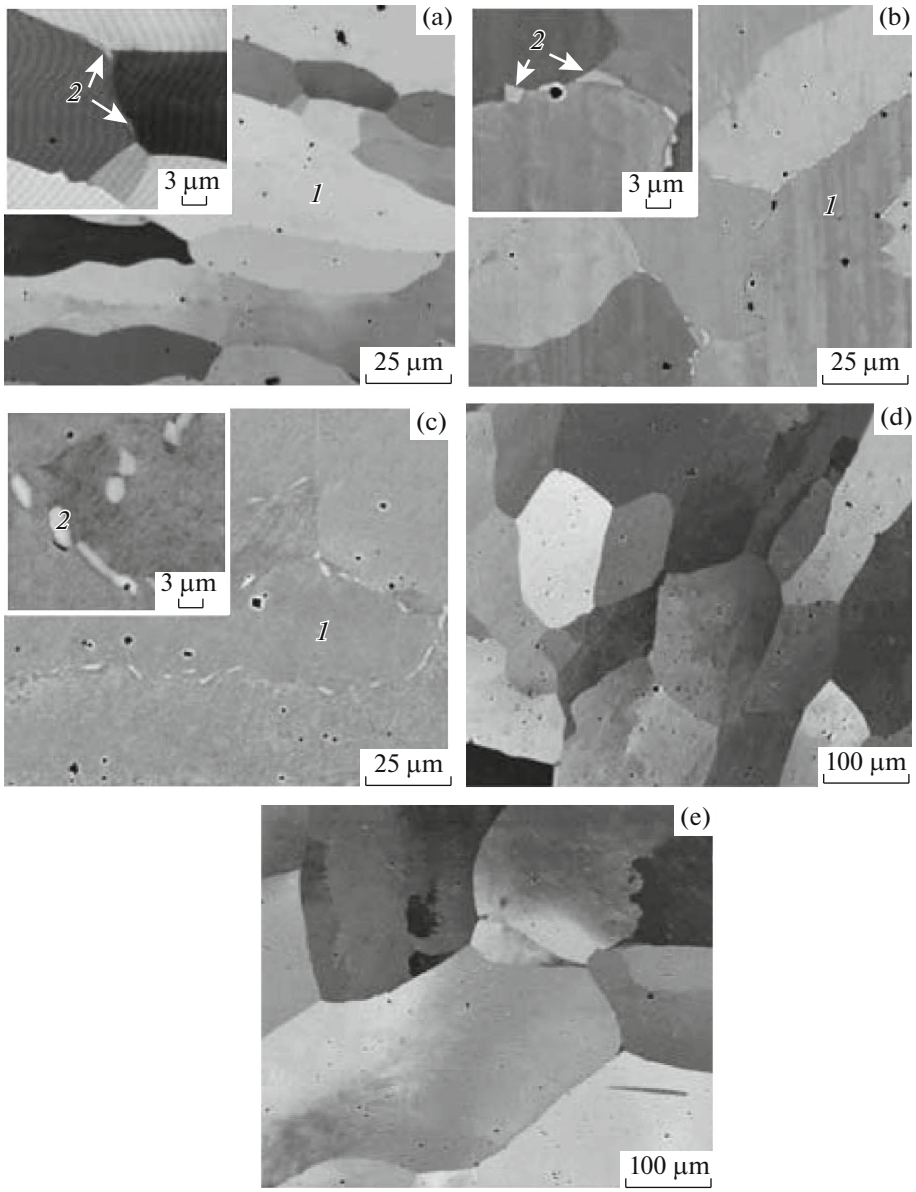

Fig. 2. Microstructure of the $CoCrFeNiMnV_{0.25}$ alloy after heating at different temperatures and subsequent holding for 24 h. SEM images: (a) 700, (b) 800, (c) 900, (d) 1000, (e) 1100°C. The γ and σ phases are denoted *1* and *2*, respectively.

diffraction analysis did not reveal its change compared to the cast state. Similar changes were observed for the $CoCrFeNiMnV_{0.75}$ and $CoCrFeNiMnV_1$ alloys. After annealing the $CoCrFeNiMnV_{0.5}$ alloy at 700°C, fine particles of the σ phase precipitate at the grain boundaries of the γ phase (Fig. 3a, *2* in the inset at a higher magnification). The initial coarse particles (Fig. 3a, *2* in the main field) do not change compared to the cast state. After annealing the $CoCrFeNiMnV_{0.5}$ alloy at temperatures in the range of 800–1000°C (Figs. 3b–3d), the precipitation of particles of a lenticular shape is observed in the γ phase. The chemical composition of the lenticular particles corresponds to the composition of coarse particles of the σ phase. With increasing annealing temperature, the lenticular particles become coarser, their amount varies nonmonotonically, and the maximum amount corresponds to 900°C (Fig. 3c). The plates are connected with the matrix by the orientation relationships $(220)_\gamma \| (\bar{1}10)_\sigma$, $[\bar{2}\,\bar{2}\,0]_\gamma \| [\bar{1}\,\bar{1}\,3]_\sigma$, $(00\bar{2})_\gamma \| (332)_\sigma$, and $[\bar{2}\,\bar{2}\,0]_\gamma \| [\bar{1}\,\bar{1}\,3]_\sigma$ and are oriented predominantly along three directions inclined at angles of 60° relative to each other [10]. The presence of precipitates of the σ phase at the boundaries of γ grains should also be noted. After annealing at 1100°C, no plate-shaped particles are observed (Fig. 3e). With increasing annealing temperature of the $CoCrFeNiMnV_{0.5}$ alloy, there is a stable tendency of the shape of particles of the σ phase to

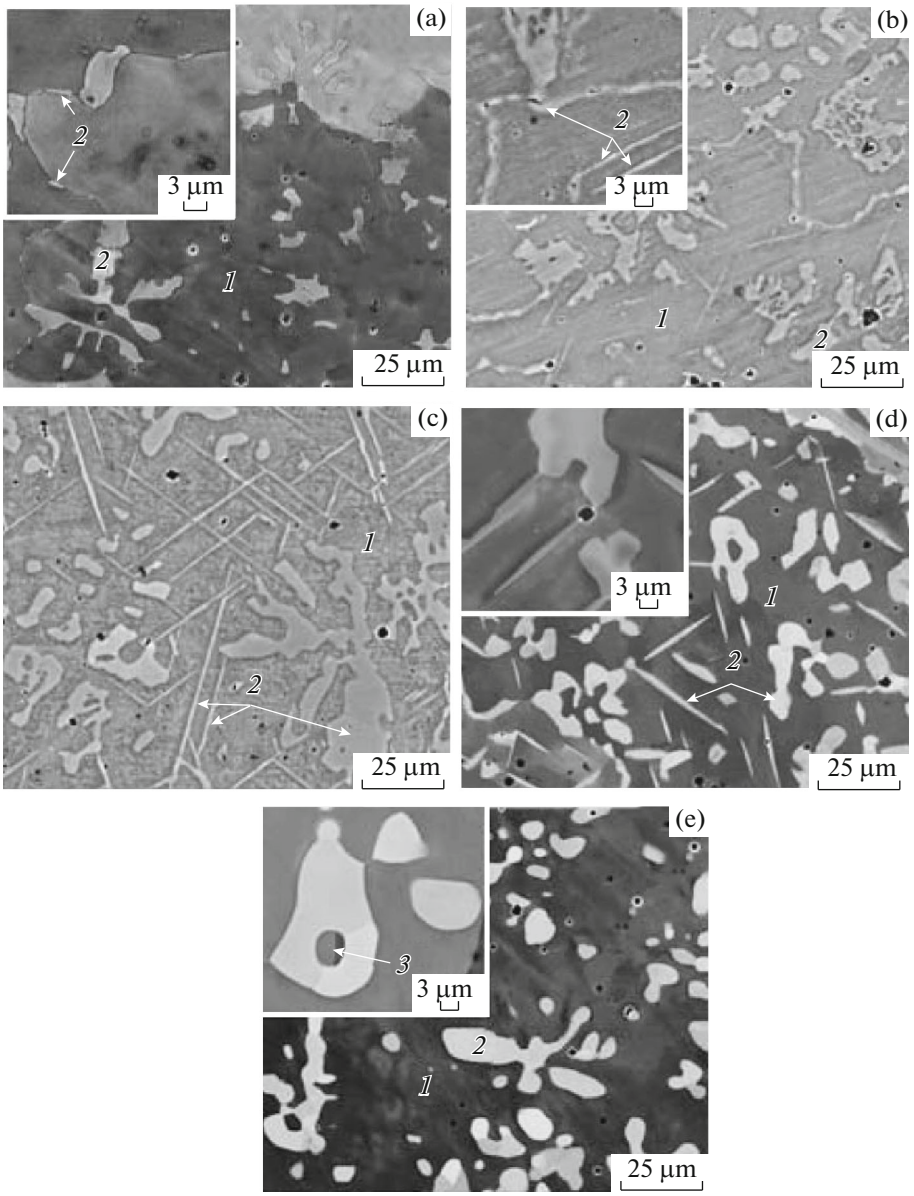

Fig. 3. Microstructure of the $CoCrFeNiMnV_{0.5}$ alloy after heating at different temperatures and subsequent holding for 24 h. SEM images: (a) 700, (b) 800, (c) 900, (d) 1000, (e) 1100°C. (*1*, *3*) γ phase; (*2*) σ phase.

simplify and particles of the γ phase to form inside the σ phase. It should be noted that, at all annealing temperatures, regions of the γ phase are retained within the particles of the σ phase.

Figure 4 shows the microstructure of the $CoCrFeNiMnV_{0.5}$ alloy after heat treatment. Annealing at 700°C (Fig. 4a) leads to significant changes in the microstructure of the alloy. In the coarse particles of the σ phase, fine plate-shaped particles of the γ phase precipitate, forming a microstructure resembling pearlite. The precipitation of the γ particles is observed predominantly in the center of the σ particles; the perimeter remains free of the precipitates. A similar microstructure is observed after annealing at 800°C (Fig. 4b). However, the shape of particles of the γ phase within the σ phase changes and approaches an equiaxed shape, apparently due to the occurrence of the process of spheroidization. In the matrix γ phase, lenticular particles of the σ phase are formed. Similar lenticular particles are seen after annealing at 900°C (Fig. 4c). In the coarse particles of the σ phase, the almost equiaxed γ particles are observed. After annealing at 1000°C (Fig. 4d) and 1100°C (Fig. 4e), no lenticular particles are observed. As a result, a microstructure with strongly curved interphase boundaries is formed due to the coalescence of particles of the γ phase that were present in the matrix σ phase. It is of interest that twins are observed in particles of the

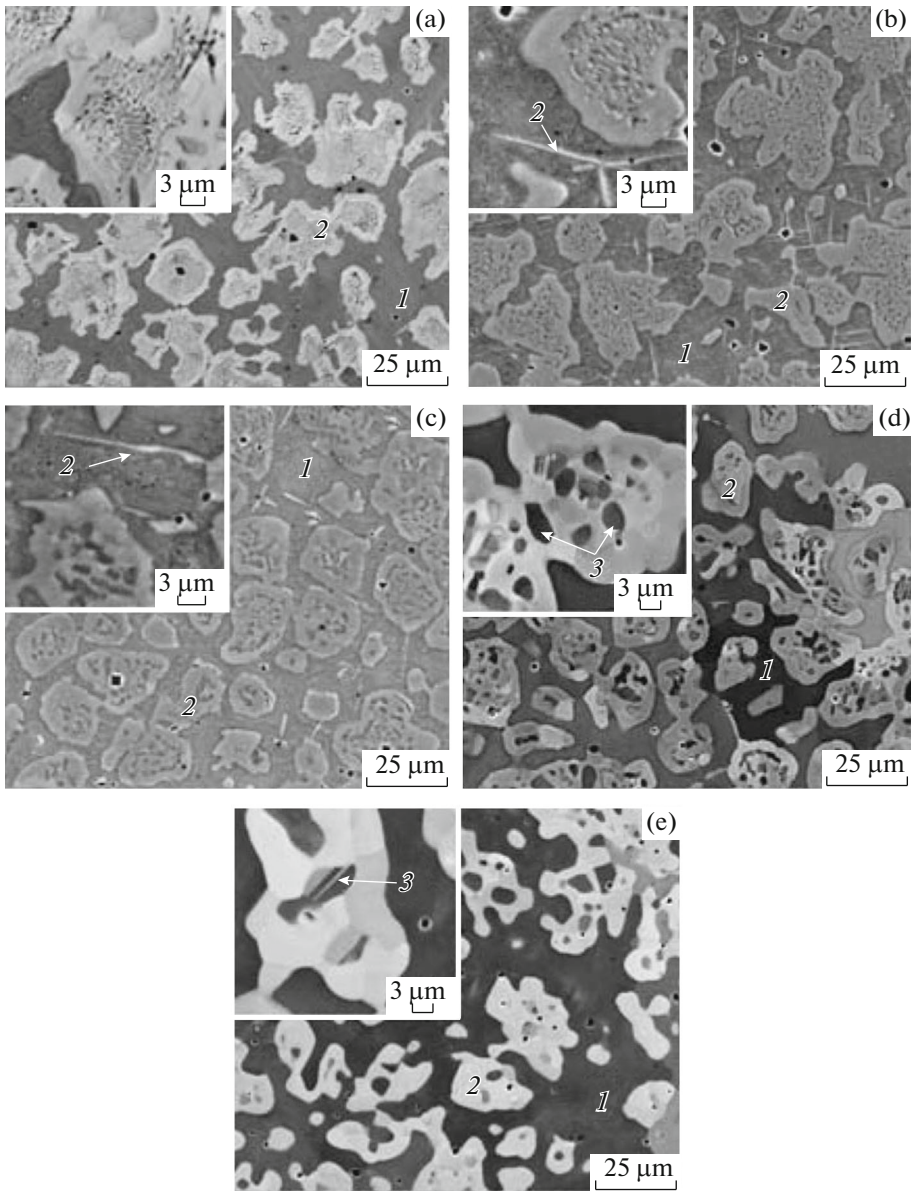

Fig. 4. Microstructure of the $CoCrFeNiMnV_{0.75}$ alloy after heating at different temperatures and subsequent holding for 24 h. SEM images: (a) 700, (b) 800, (c) 900, (d) 1000, (e) 1100°C. (*1*, *3*) γ phase; (*2*) σ phase.

γ phase (*3* in Fig. 4e) located in the σ phase; whereas, in the σ particles, grain boundaries are formed (Fig. 4e, inset).

The microstructure of the $CoCrFeNiMnV_1$ alloy after annealing at different temperatures is presented in Fig. 5. Annealing at 700°C does not lead to significant changes in the microstructure of the alloy compared to the cast state (cf. Figs. 5a and 1d). Heating to 800°C leads to a coarsening of the platelike structure of the γ particles in the σ matrix and its spheroidization (Fig. 5b). Inside the interlayers of the γ phase, dark particles of the fine-dispersed σ phase precipitate; because of their small size, they were only identified after annealing at 900°C, when they became somewhat coarser (Fig. 5d). At $T = 900$°C (Fig. 5c), the spheroidization of the particles of the γ phase is almost completed and the microstructure represents grains of the σ phase in which spheroidized particles of the γ phase are located. At the boundaries of grains of the σ phase, precipitates of the primary γ phase are located, in which equiaxed and platelike particles of the σ phase can be seen (Fig. 5d). After annealing at a temperature of 1000°C (Fig. 5e), equiaxed particles of the γ phase become coarser; no precipitation of the σ phase in the interlayers of the γ phase occurs. Upon a further increase in the annealing temperature to 1100°C, because of the development of the processes of coalescence and spheroidization, the microstruc-

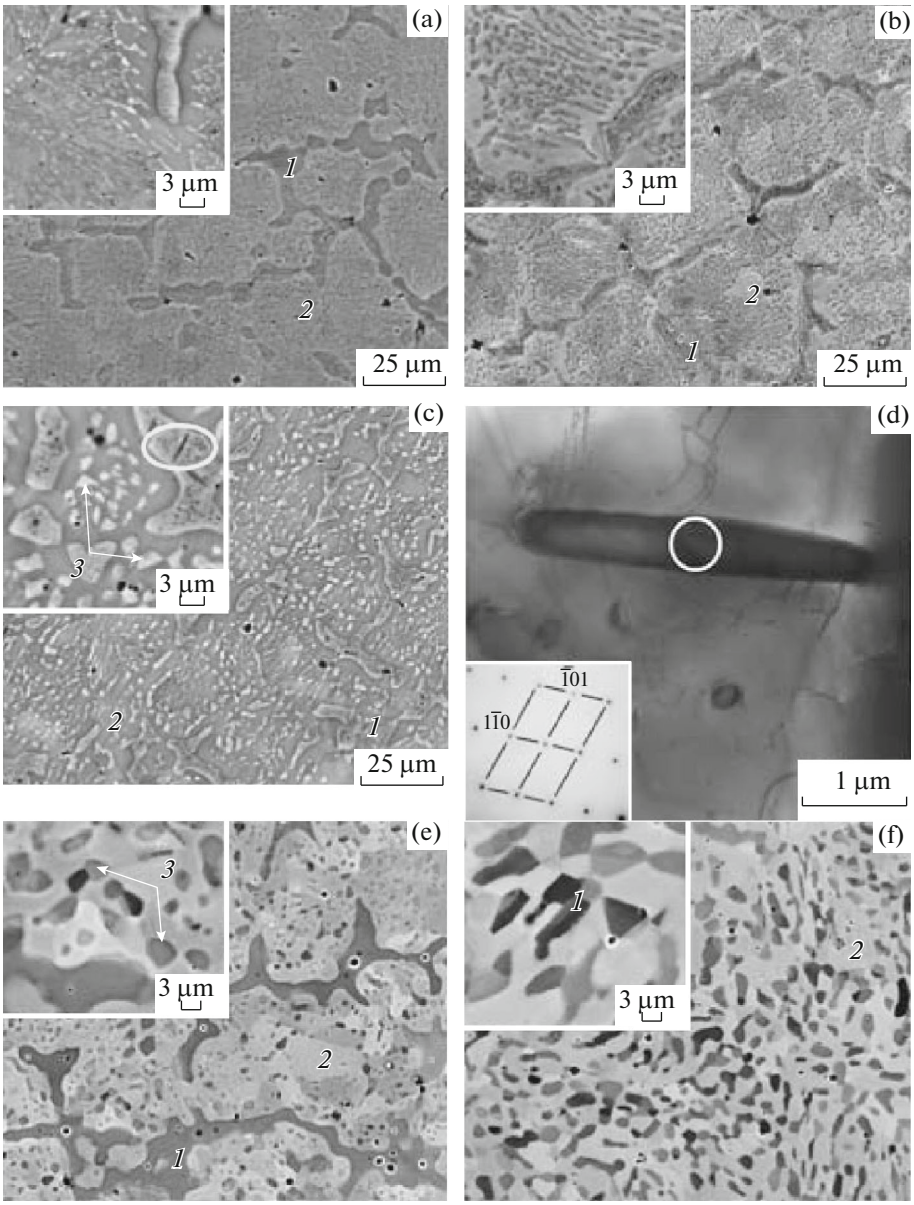

Fig. 5. Microstructure of the $CoCrFeNiMnV_1$ alloy after heating at different temperatures and subsequent holding for 24 h: (a) 700, (b) 800, (c), (d) 900, (e) 1000, (f) 1100°C. (a–c, e, f) SEM images. (d) TEM image and electron-diffraction pattern corresponding to the region outlined by an oval in Fig. 5c. (*1*, *3*) γ phase; (*2*) σ phase.

ture is transformed into a microduplex-type structure (Fig. 5f), which morphologically does not inherit the microstructure of the cast state.

The chemical composition of phases that arise in the $CoCrFeNiMnV_x$ alloys ($x = 0.25, 0.5, 0.75, 1$) was analyzed using the EDS method. Figure 6 shows the dependences of the total content of chromium and vanadium in the γ and σ phases on the annealing temperature. The σ phase is strongly enriched in chromium and vanadium. The total concentration of chromium and vanadium is approximately the same in all alloys (except the $CoCrFeNiMnV_{0.25}$ alloy) and is in the range of 35–40 at % (Fig. 6). The total content of chromium and vanadium in the γ phase also only weakly depends on the vanadium concentration in the alloys and is about 23–27 at % (Fig. 6). The γ and σ phases contain the other elements (Co, Fe, Ni, and Mn) in approximately equal concentrations. Heat treatment exerts a significant effect on the chemical composition of phases. As can be seen in Fig. 6, annealing at 700°C does not lead to significant changes in the composition of the phases. With an increase in annealing temperature to 800 and 900°C, the total content of chromium and vanadium in the γ solid solution decreases; in the σ phase, the content increases. The further increase in the annealing tem-

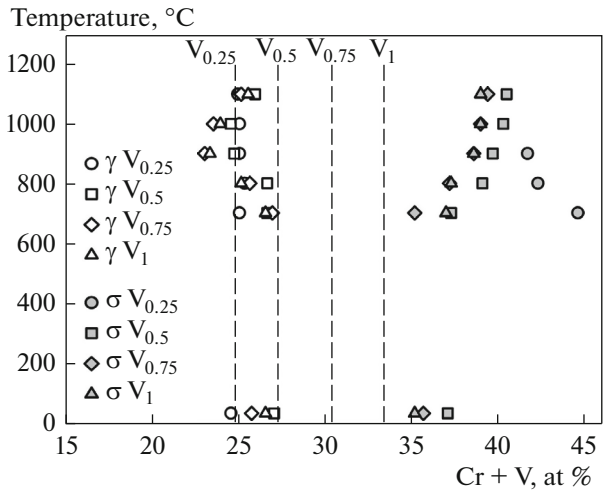

Fig. 6. Dependence of the total content of chromium and vanadium in the γ phase (white symbols) and σ phase (gray symbols) of the $CoCrFeNiMnV_x$ alloys (x = 0.25, 0.5, 0.75, 1) on the annealing temperature. Content of chromium and vanadium in the alloys is indicated by dashed lines.

perature to 1000 and 1100°C does not lead to significant changes in the composition of the σ phase, while in the γ phase, an increase in the total content of chromium and vanadium is observed. It can also be noted that the chemical composition of the σ phase in the $CoCrFeNiMnV_{0.25}$ alloy differs from that in the other alloys; the total content of chromium and vanadium in the σ phase is maximum after annealing at a temperature of 700°C (44.6 at %) and gradually decreases with increasing annealing temperature, which approaches the amount that is typical of the σ phase in alloys with higher vanadium content. The difference in the composition of the σ phase in different alloys is caused by the fact that, in the $CoCrFeNiMnV_{0.25}$ alloy, the σ phase probably only precipitates upon annealing, whereas in other alloys, the σ phase is already present in the initial cast state.

The changes in the volume fraction of the σ phase and the microhardness in the $CoCrFeNiMnV_x$ alloys after annealing at different temperatures compared to the cast state are presented in Fig. 7. The curves demonstrate a substantial dependence of the volume fraction of the σ phase (Fig. 7a) and the microhardness (Fig. 7b) on the vanadium content in alloys in the cast and annealed states. As the vanadium content increases, the volume fraction of the σ phase and the microhardness increase. The dependences of the amount of the σ phase and of the microhardness on the vanadium content are not directly proportional to vanadium concentration, but the greater its content in the alloy, the higher the increase. As was noted above, the annealing at 700° of the alloy with $V_{0.25}$ leads to the formation of the σ phase, but its volume fraction is insignificant, just as the effect on the microhardness.

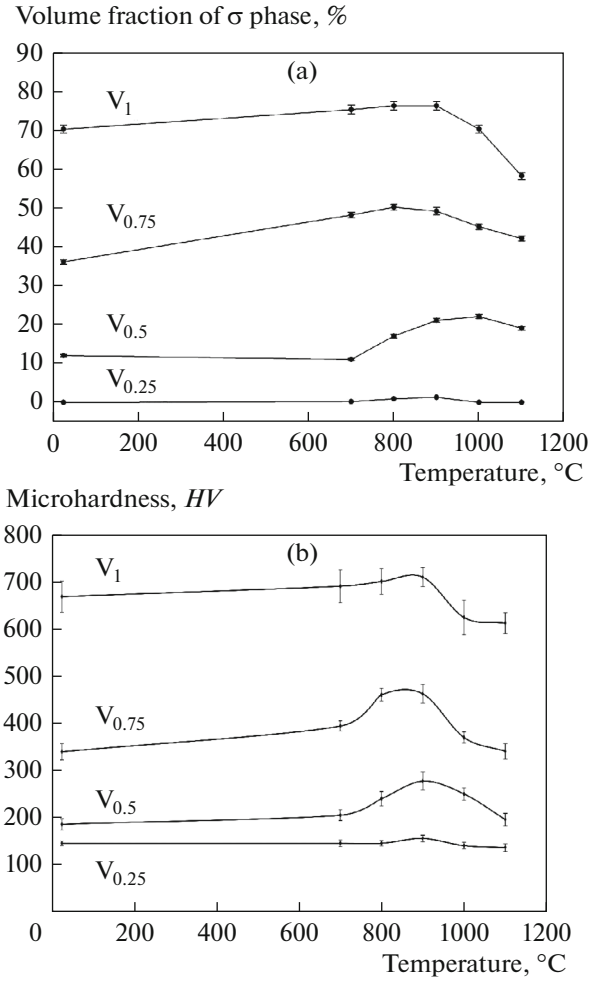

Fig. 7. Dependence of (a) volume fraction of the σ phase and (b) microhardness of $CoCrFeNiMnV_x$ alloys (x = 0.25, 0.5, 0.75, 1) on annealing temperature.

In the other alloys, annealing led to a significant change in the volume fraction of the σ phase, the maximum of which was observed in the range of annealing temperatures of 800–1000°C depending on the vanadium content. In alloy with $V_{0.5}$, the maximum was observed after annealing at 1000°C; in alloys with $V_{0.75}$ and V_1 the maximum was observed at somewhat lower temperatures (800–900°C). After reaching the maximum, the volume fraction of the σ phase decreased in all the alloys. The change in the microhardness of the alloys after annealing in general correlated with the change in the volume fraction of the σ phase. However, the observed maxima look clearer (especially for the alloys with $V_{0.5}$ and $V_{0.75}$) than the peaks in the change of the volume fraction of the σ phase.

Additionally, a study of the $CoCrFeNiMnV_x$ alloys (x = 0, 0.25, 0.5, 0.75, 1) was performed using the DSC method. Based on the results of this study, a polythermal section of the phase diagram of alloys of the CoCrFeNiMn–V system was constructed (Fig. 8)

taking into account the results of the structural studies of the alloys as well. For the $CoCrFeNiMnV_x$ alloys ($x = 0.5, 0.75, 1$), the temperatures of the liquidus, solidus, and solvus of the σ phase were determined. The temperatures of the phase transformations in these alloys only weakly depend on their composition. The complete dissolution of the σ phase in these alloys is possible in a narrow range of temperatures of 1200–1250°C. In the CoCrFeNiMn and $CoCrFeNiMnV_{0.25}$ alloys, only the temperatures of liquidus and solidus were determined upon the DSC studies, probably because of the low volume fraction of the σ phase in these alloys and possibly because of the slow kinetics of its precipitation. Therefore, the boundary between the γ (fcc) and γ + σ fields (of existance) in the phase diagram was drawn tentatively (dashed line). The fact (established in the present paper) of the presence of the σ phase in the $CoCrFeNiMnV_{0.25}$ alloy after annealing at temperatures in the range of 700–900°C and the absence of this phase after annealing at 1000–1100°C was also taken into account. In addition, the known data on the precipitation of the σ phase in the CoCrFeNiMn alloy after annealing at 600–700°C and on the single-phase γ structure after annealing at 900–1000°C were taken into account [17–19]. The phase diagram is characterized by a wide field of the γ solid solution, which is sharply narrowed as the molar concentration of vanadium increases from 0 to 0.5. The broadening of the γ + σ region is assumed to be due to an increase in the volume fraction of the σ phase, which is confirmed by microstructural studies (Fig. 7a).

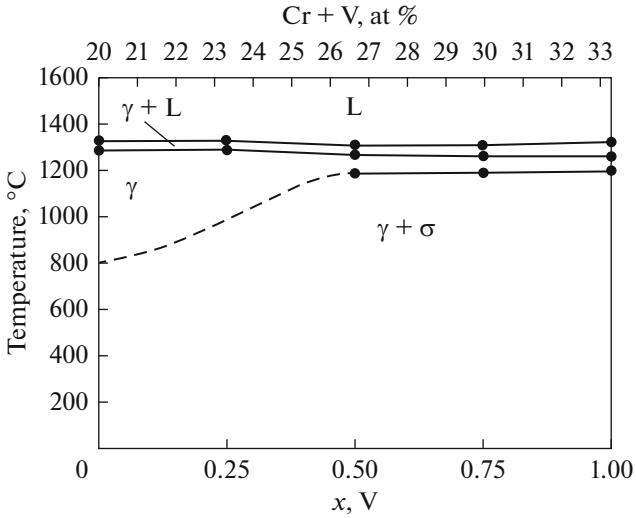

Fig. 8. Schematic phase diagram of CoCrFeNiMn-V alloys, which was constructed using DSC curves with taking into account the data of microstructural studies.

DISCUSSION

The above results show that the structure of the $CoCrFeNiMnV_x$ alloys ($x = 0.25; 0.5; 0.75; 1$), namely, the volume fraction of arising phases, their morphology, and the composition depend not only on the vanadium content, as was shown in the previous paper [10], but also on the annealing temperature. The structural changes are caused by phase transformations, i.e., the reactions of the precipitation of phases $\sigma \rightarrow \gamma$ and $\gamma \rightarrow \sigma$. The latter reaction, unlike the former one, is well known [20] and was observed in austenitic steels and superalloys. The formation of the σ phase takes place in all of the studied alloys; its volume fraction increases with increasing vanadium concentration, which is directly related to an increase in the content of the σ-forming elements (Cr and V) to 34 at % (Fig. 6). The change in its volume fraction with increasing annealing temperature has a more complicated character: first, the volume fraction increases to the temperature of 900°C, then decreases (Fig. 7a). The change in the volume fraction correlates well with the change in the microhardness (Fig. 7b).

Let us consider the formation of the microstructure of the alloys depending on the vanadium content and annealing temperature. According to the presented phase diagram of the CoCrFeNiMn–V system (Fig. 8), all of the alloys are characterized by a narrow region of crystallization; the temperature range between the solidus and solvus is only wide at small concentrations of vanadium. Beginning with the concentration of $V_{0.5}$, the difference in the temperatures of solidus and solvus does not exceed 70 K. Since the cooling rate of ingots was quite high (50 K/s up to 800°C), the crystallization resulted in the formation of a metastable structure in the alloys. Indeed, in the $CoCrFeNiMnV_{0.25}$ alloy, the σ phase is not detected in the cast state (Fig. 1a) and after quenching from temperatures of 1000 and 1100°C (Figs. 2d, 2e) but appears after heating in the range of temperatures of 700–900°C, whereas in the alloys with a high vanadium content at lower annealing temperatures, the precipitation of the γ phase from the σ phase due to its supersaturation by the γ-forming elements is observed (Fig. 6). A similar change in the microstructure was noted in [21] upon studying the decomposition of the supersaturated solid solutions in Ni–Cr and Cu–Ti systems. At certain degrees of overcooling, a pearlite-like microstructure was observed close to the microstructure observed in the present paper. As a result, the arising plates of the γ phase are unstable; we can clearly see the curvature of boundaries and the appearance of constrictions (Fig. 1f). The spheroidization and coalescence are activated with increasing annealing temperature, which leads to the formation of rounded particles.

Meanwhile, beginning with the temperature of 700°C, the opposite reaction $\gamma \rightarrow \sigma$ gradually occurs, which is caused by the change in the solubility of the σ-forming elements in the γ phase. Two morphological types of particles of the σ phase are formed, i.e., equiaxed and lenticular. In this case, there is an anal-

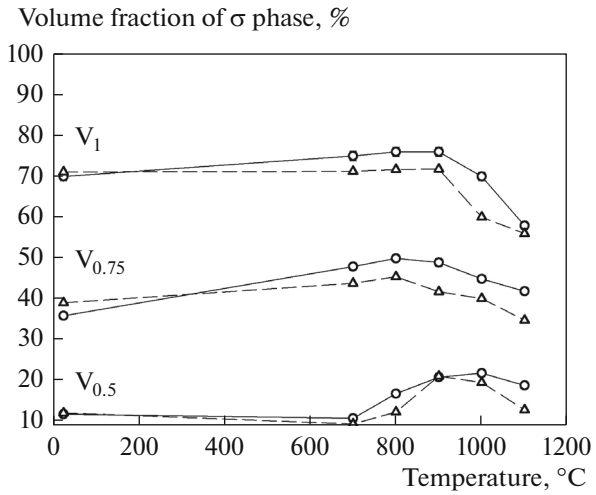

Fig. 9. Dependence of volume fraction of σ phase on annealing temperature for $CoCrFeNiMnV_x$ alloys ($x = 0.5$; 0.75; 1): (Δ) dependence predicted according to the lever rule; (○) experimental data.

ogy with the formation of the σ particles in austenitic steels [21]. According to [20], the formation of the σ phase in these steels occurs by the transformation of δ ferrite, or the σ phase directly precipitates from the γ solid solution [21]. In the present paper, apparently, the formation of δ ferrite is prevented because of a high content of γ-stabilizers (Mn, Ni, Co), which expand the region of existence of the γ phase. In the $CoCrFeNiMnV_{0.25}$ alloy, the σ phase precipitates at grain boundaries. Such equiaxed precipitates of the σ phase were observed in [22] during the study of the Fe–Cr–Ni–Mo alloy. The authors of [22] have shown that the precipitation of particles of the σ phase at the grain boundaries of the γ solid solution and in the bulk of grains occurs at an aging temperature of 815°C for 36 h. The σ phase precipitated in the bulk of grains has a needle-like shape; the same shape was observed in the $CoCrFeNiMnV_{0.5}$ alloy after annealing at 800°C and above. An attempt to explain the mechanism of the formation of the σ phase from austenite was made in [21], where it was assumed that the nucleation of the σ phase is favored by the segregation of chromium at grain boundaries. In our case, after the exhaustion of the segregated chromium, the growth of the σ phase is promoted by vanadium, which comes through the grain boundaries and interphase boundaries.

The specific features of diffusion in HEAs can play a certain role in the formation of the microstructure of investigated alloys upon annealing. It is known that the diffusion in the high-entropy solid solutions is slow as compared to conventional alloys [23]. We can assume that, in the multicomponent σ phase of $CoCrFeNiMnV_x$ alloys, the diffusion will also be slow. Therefore, the mass transfer to large distances will be difficult. In this regard, it should be noted that a maximum amount of the lenticular σ particles precipitated in the γ phase is observed in the $CoCrFeNiMnV_{0.5}$ alloy (Figs. 3c, 3d). In this alloy, the distance between particles of the σ phase is significantly larger than that in the alloys with high vanadium content. Correspondingly, it is difficult to provide the leveling-off of the chemical composition between phases because of a large diffusion path. Similarly, the precipitation of the γ particles in the σ particles is observed in the $CoCrFeNiMnV_{0.75}$ alloy (Figs. 4a, 4b). On the one hand, in the alloy with $V_{0.75}$, the transverse size of particles of the σ phase is much greater than that in the $CoCrFeNiMnV_{0.5}$ alloy, which makes it difficult the diffusion of elements from the center of a particle to the interphase boundary. On the other hand, in the cast structure of the alloy with $V_{0.75}$, there are no dispersed γ particles in the σ phase, which provide the high availability of the interphase boundaries. The presence of a layer free of γ particles along the perimeter of the particles of the σ phase in the $CoCrFeNiMnV_{0.5}$ alloy should also be noted, the formation of which is caused by the achievement of a composition of the phase that is close to equilibrium due to diffusion through the interphase boundary at the thickness of this layer.

The phase transformations that occur upon heat treatment change the volume fractions of phases in the $CoCrFeNiMnV_x$ alloys, as is shown in Fig. 7a. The change in the volume fractions of phases upon heat treatment should be associated with the change in their chemical composition, namely, in the total concentration of chromium and vanadium (Fig. 6). Let us compare the volume fractions of phases, which were obtained experimentally and were calculated using the lever rule [10] (Fig. 9). The calculated values of the volume fraction of the σ phase in different states are indicated in Fig. 9 by triangles, while the experimental data are indicated by circles. Obviously, there is rather good qualitative agreement between the experimental and predicted trends in the change of the volume fraction of the σ phase. For example, the experimental and predicted temperatures that correspond to the maxima of the volume fraction of the σ phase for each alloy completely coincide. Some discrepancy in the obtained absolute values of the volume fractions can apparently be explained by (i) the different efficiency of chromium and vanadium in the stabilization of the σ phase [10] and (ii) by the experimental errors upon the determination of the composition and volume fractions of phases. However, on the whole, it can be concluded that the change in the volume fractions of the fcc and σ phases in the $CoCrFeNiMnV_x$ alloys ($x = 0.5$, 0.75, 1) upon heat treatment occurs due to the changes in the total content of σ-forming elements of chromium and vanadium in the phases according to the lever rule.

The changes in the volume fraction of the σ phase are expected to inevitably affect the hardness of the $CoCrFeNiMnV_x$ alloys, which follows from a similar

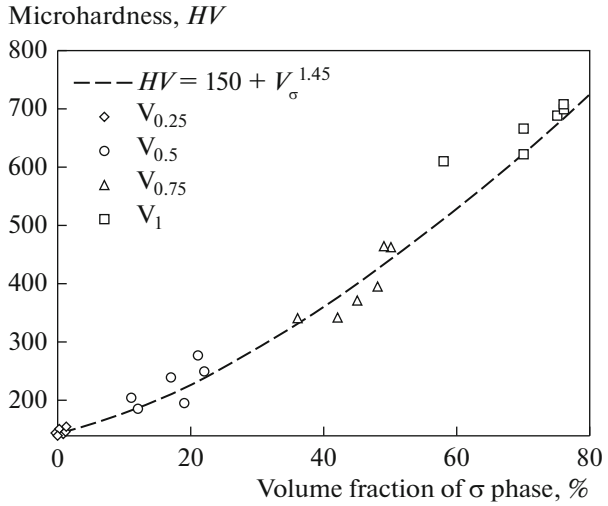

Fig. 10. Dependence of microhardness on the volume fraction of the σ phase for $CoCrFeNiMnV_x$ alloys (x = 0.25, 0.5, 0.75, 1).

character of the change in the volume fraction of the σ phase and microhardness depending on the annealing temperature (Figs. 7a and 7b, respectively). The previous study of the $CoCrFeNiMnV_x$ alloys in the cast state and after annealing at 1000°C with subsequent slow cooling revealed the presence of the power dependence between the volume fraction of the σ phase and the microhardness [10]. An analysis of the results obtained in the present paper confirmed the presence of the power dependence; the experimental data are well approximated by a power function (Fig. 10). The exponent obtained in the present paper is equal to 1.45, which completely coincides with the results of the previous analysis [10]. The constants that correspond to the hardness of the γ phase are close to 150 and 142.4 *HV*, respectively. It should be noted that, in the case of alloys that consist of two phases with significant volume fractions and different mechanical characteristics, a linear ratio between the volume fractions of phases and the strength, i.e., the so-called rule of mixture, is usually fulfilled. In the case under consideration, there is observed a positive deviation from this rule, i.e., the exponent in the power dependence is significantly higher than 1. Apparently, this deviation indicates that an increase in the volume fraction of the σ phase simultaneously leads to an additional change in the parameters of the microstructure that provide a strengthening of the alloys. It can be assumed that this additional strengthening is also caused by the observed $\sigma \rightarrow \gamma$ and $\gamma \rightarrow \sigma$ phase transformations, which significantly increase the dispersion of the microstructure.

Thus, the results of this study show that, in the high-entropy alloys of the CoCrFeNiMn–V system, the structure and properties can be controlled by changing the concentrations of alloying elements (vanadium) and by heat treatment. The possible structures can be quite different; from the very ductile γ solid solution to the structure with the matrix intermetallic σ phase, which is characterized by a high hardness and brittleness. We hope that the relationships established in this paper between the composition, regimes of treatment, structural parameters, and properties of the CoCrFeNiMn–V alloy will make it possible to produce alloys with desired characteristics owing to the control of their composition and microstructure. A similar approach can also be applied to other systems of high-entropy alloys, which are promising materials for practical applications.

CONCLUSIONS

In this paper, the structure and microhardness of the $CoCrFeNiMnV_x$ alloys (x = 0.25, 0.5, 0.75, 1) have been studied in the cast state and after annealing at temperatures in the range of 700–1100°C. Based on the studies carried out, we can draw the following conclusions.

(1) The structure of the alloys, i.e., the volume fraction of phases (fcc solid solution (γ) and intermetallic σ phase), their morphology, and composition, depends on the vanadium content and annealing temperature. It has been shown that the structural changes upon annealing are caused by phase transformations, predominantly by the reactions of the precipitation of phases ($\sigma \rightarrow \gamma$ and $\gamma \rightarrow \sigma$).

(2) It has been found that the formation of the σ phase takes place in all of the alloys studied, and its volume fraction increases with increasing vanadium content. The volume fraction of the σ phase varies nonmonotonically with increasing annealing temperature; first the volume fraction increases, then it decreases. It has been shown that these changes upon annealing occur due to the changes in the total content of σ-forming elements (chromium and vanadium) in accordance with the lever rule.

(3) The method of DSC analysis makes it possible to determine the temperatures of the liquidus, solidus, and solvus of the σ phase. The solvus temperature was only determined for the $CoCrFeNiMnV_x$ alloys with x = 0.5, 0.75, 1. It has been found that the complete dissolution of the σ phase in these alloys is possible in a narrow temperatures range of 1200–1250°C.

(4) It has been shown that the microhardness of the studied alloys increases significantly with increasing vanadium content, varies with annealing temperature, and correlates with the change in the volume fraction of the σ phase. The power dependence between the microhardness and the volume fraction of the σ phase with an exponent equal to 1.45 has been found.

ACKNOWLEDGMENTS

The work was supported by the Russian Science Foundation (project no. 14-19-01104).

REFERENCES

1. J.-W. Yeh, S.-K. Chen, S.-J. Lin, J.-Y. Gan, Ts.-Sh. Chin, T.-Ts. Shun, Ch.-H. Tsau, and Sh.-Y. Chang, "Nanostructured high-entropy alloys with multiple principle elements: Novel alloy design concepts and outcomes," Advan. Eng. Mater. **6**, 299–303 (2004).
2. O. N. Senkov, J. D. Miller, D. B. Miracle, and C. Woodwart, "Accelerated exploration of multiprincipal element alloys with solid solution phases," Nature Commun. **6**, 6529–6529 (2015).
3. Y. P. Wang, B. Sh. Li, and Zh. F. Heng, "Solid solution or intermetallics in a high-entropy alloy," Advan. Eng. Mater. **11**, 641–644 (2009).
4. S. Singh, N. Wanderka, B. S. Murty, U. Glatzel, and J. Banhart, "Decomposition in multi-component AlCoCrCuFeNi high-entropy alloy," Acta Mater. **59**, 182–190 (2011).
5. M. V. Ivchenko, V. G. Pushin, A. N. Uksusnikov, N. I. Kourov, and N. Wanderka, "Specific features of cast high-entropy AlCrFeCoNiCu alloys produced by ultrarapid quenching from the melt," Phys. Met. Metallogr. **114**, 503–513 (2013).
6. M. V. Ivchenko, V. G. Pushin, A. N. Uksusnikov, and N. Wanderka, "Microstructure features of high-entropy equiatomic cast AlCrFeCoNiCu alloys," Phys. Met. Metallogr. **114**, 514–520 (2013).
7. M.-H. Tsai, K.-Y. Tsai, C.-W. Tsai, C. Lee, C.-C. Juan, and J.-W. Yeh, "Criterion for sigma phase formation in Cr- and V- containing high-entropy alloys," Mater. Res. Lett. **1**, 207–212 (2013).
8. S.-T. Chen, W.-Y. Tang, Y.-F. Kuo, S.-Y. Chen, C.-H. Tsau, T.-T. Shun, and J.-W. Yeh, "Microstructure and properties of age-hardenable $Al_xCrFe_{1.5}MnNi_{0.5}$ alloys," Mater. Sci. Eng., A. **527**, 5818–5825 (2010).
9. G. A. Salishchev, M. A. Tikhonovsky, D. G. Shaysultanov, N. D. Stepanov, A. V. Kuznetsov, I. V. Kolodiy, A. S. Tortika, and O. N. Senkov, "Effect of Mn and V on structure and mechanical properties of high entropy alloys based on FeCrCoNi system," J. Alloys Compd. **591**, 11–21 (2014).
10. N. D. Stepanov,D. G. Shaysultanov, G. A. Salishchev, M. A. Tikhonovsky, E. E. Oleynik, A. S. Tortika, and O. N. Senkov, "Effect of V content on microstructure and mechanical properties of the $CoCrFeMnNiV_x$ high entropy alloys," J. Alloys Compd. **628**, 170–185 (2015).
11. M.-R. Chen, S.-J. Lin, J.-W. Yeh, S.-K. Chen, Y.-S. Huang, and M.-H. Chuang, "Effect of vanadium addition on the microstructure, hardness and wear resistance of $Al_{0.5}CoCrCuFeNi$ high-entropy alloy," Metall. Mater. Trans., A **37**, 1363–1369 (2006).
12. D. G. Shaysultanov, N. D. Stepanov, A. V. Kuznetsov, G. A. Salishchev, and O. N. Senkov, "Phase composition and superplastic behavior of a wrought AlCrCuNiFeCo high-entropy alloy," JOM **65**, 1815–1828 (2013).
13. E. O. Hall and S. H. Algie, "The sigma phase," Int. Mater. Rev. **11**, 161–88 (1966).
14. F. F. Khimushin, *Stainless Steels* (Metallurgizdat, Moscow, 1963) [in Russian].
15. L. C. Tsao, C. S. Chen, and C. P. Chu, "Age hardening reaction of the $Al_{0.3}CrFe_{1.5}MnNi_{0.5}$ high entropy alloy," Mater. Design. **36**, 854–858 (2012).
16. M.-Y. Tsai, H. Yuan, G. Cheng, W. Xu, W. W. Jian, M.-H. Chuang, C.-C. Juan, A.-C. Yeh, S.J. Lin, and Y. Zhu, "Significant hardening due to the formation of a sigma phase matrix in a high entropy alloy," Intermetallics **33**, 81–86 (2013).
17. B. Schuh, F. Mendez-Martin, B. Völker, E. P. George, H. Clemens, R. Pippan, and A. Hohenwarter, "Mechanical properties, microstructure and thermal stability of a nanocrystalline CoCrFeMnNi high-entropy alloy after severe plastic deformation," Acta Mater. **96**, 258–268 (2015).
18. E. J. Pickering, R. Muñoz-Moreno, H. J. Stone, and N. G. Jones, "Precipitation in the equiatomic high-entropy alloy CrMnFeCoNi," Scr. Mater. **113**, 106–109 (2016).
19. N. D. Stepanov, D. G. Shaysultanov, M. S. Ozerov, S. V. Zherebtsov, and G. A. Salishchev, "Second phase formation in the CoCrFeNiMn high entropy alloy after recrystallization annealing," Mater. Lett. **185**, 1–4 (2016).
20. C.-C. Hsieh and W. Wu, "Overview of intermetallic sigma (σ) phase precipitation in stainless steels," ISRN Metall. **2012**, Article ID 732471. (2012)
21. A. A. Popov, A. S. Bannikova, and S. V. Belikov, "Precipitation of the sigma phase in high-alloy austenitic chromium–nickel–molybdenum alloys," Phys. Met. Metallogr. **108**, 586–592 (2009).
22. A. A. Baranov, *Phase Transformation and Thermal Cycling of Metals* (Kiev, Naukova Dumka, 1974) [in Russian].
23. K. Y. Tsai, M. H. Tsai, and J.-W. Yeh, "Sluggish diffusion in CoCrFeMnNi high entropy alloys," Acta Mater. **61**, 4887–4897 (2013).

Translated by O. Golosova